Available online at www.dergipark.org.tr/en

INTERNATIONAL ADVANCED RESEARCHES and ENGINEERING JOURNAL

Journal homepage: www.dergipark.org.tr/en/pub/iarej

e-ISSN: 2618-575X

International Open Access

Volume 05
Issue 03

December, 2021

Research Article

Explicit dynamics finite element analyses of asymmetrical roll bending process

Tuncay Kamaş [a,*] ***and Müfit Sarıkaya*** [a]

[a]*Akyapak Makina A.Ş Research and Development Center. Hasanağa Osb Mah. Hosab Sanayi Cad. No:62 Nilüfer / Bursa, Türkiye*

ARTICLE INFO

Article history:
Received 24 May 2021
Revised 10 September 2021
Accepted 14 October 2021

Keywords:
Elliptically curved plates
Finite element analysis
Harmonic response

ABSTRACT

In this article, results obtained from a preliminary study that contains a set of explicit dynamics finite element analyses of a metal plate bending process are presented through 3D asymmetrical three roller models. ANSYS Ls-Dyna explicit dynamics finite element (ED-FEA) preprocessor and solver were used to carry out dynamic simulations. Explicit dynamics of a low-velocity process such as the roll-bending of a metal plate is a computationally expensive method. Since plastic deformation occurs on the plate in addition to elastic flexure to eventually possess a circular geometry, the plate material is considered a non-linear material. In this particular study, an aluminum plate was modeled with the Bilinear Kinematic Hardening model including plasticity parameters such as the tangent modulus. A very significant parameter called the mass scaling factor was taken into account to be able to define a specific time-step that was used to determine the computation time interval and the total temporal cost. However, exaggerated reduction of the computation time results in unphysical consequences. The results were presented before and after redesigning the lower and side rolls having a convex geometry and the peripheral velocity of upper roll rotation was decreased to minimize the distortion that occurred on the pre-bent side walls of the aluminum plate.

1. Introduction

In energy and civil engineering fields, the metal pipe industry plays a significant role and via this industry, large-diameter circular pipes can be produced with a single weld bead. The pipelines are required to flawlessly convey liquid or gas without any leakage to a long distance thanks to new technological developments on plate bending process in recent decades. Three roll pyramids [1,2] and asymmetric machines [3–5] and four roll machines [6,7] have been developed to bend plates into cylinders, tanks, and pipes. Pipe, tank, or any large-sized cylindrical metal product manufacturers commonly choose four roll plate bending machines (Figure 2) because they have better efficiency compared to three roller machines. Four roll plate bending machines can have different operation modes to be able to carry out versatile functions with two independent side rolls that can be swung upward and downward and be pivoted by a wing to be suitably located for pre-bending and bending processes.

In the literature, many outstanding theoretical and experimental researches [2,8–13] have been performed to develop analytical and empirical models as well as FEA models regarding three-roller and four-roller machines. Gandhi and Raval [2] discussed three analytical concepts for pyramid type three-roller bending process and proposed an empirical model to estimate the top roller position explicitly as a function of desired (final) radius of curvature for three-roller bending considering the contact point shift at the bottom roller plate interfaces. Tailor et-al [11] investigated the effects of top roller and of rolling speed on bending quality by using an explicit dynamic FEA model in Hypermesh/Ls-Dyna. The four roll plate bending procedures in one pass using one of the side rolls without pre-bending have been modeled more widely asymmetric-three roller models [3,5]. Gavrilescu et al. [14,15] attempted to analytically and numerically model a pyramid three roll bending process. They utilized a 2-D model in a commonly known commercial FEA software, LS-DYNA, alike many other metal-forming researchers [4,16], in the ANSYS Workbench Graphical User Interface (GUI). They also developed an analytical model to predict the vertical displacement of the inner roller to obtain the desired curvature by using geometrical and deformation compatibilities. In addition, they developed

* Corresponding author. Tel.: +90 224 280 75 00; Fax: +90 (224) 280 75 01.
E-mail addresses: tkamas@akyapak.com *(T. Kamas)*, ms@akyapak.com *(M. Sarıkaya)*
ORCID: 0000-0002-4623-5732 *(T. Kamas)*, 0000-0002-0413-6146 *(M. Sarıkaya)*
DOI: 10.35860/iarej.934544
© 2021, The Author(s). This article is licensed under the CC BY-NC 4.0 International License (https://creativecommons.org/licenses/by-nc/4.0/).

another mathematical procedure to estimate the bending force. For validation, they compared analytical model results with FEA results. Authors attempted to estimate the vertical displacement versus inner radii of the plate and versus the bending forces. In the beginning of the parametric study conducted with S235JR and S275JR steel materials at various thicknesses and the inner roller at various vertical displacements, they did not have a precise predictive model, however, the loop in the algorithm using the regression models increased the precision further in each iteration.

Fu et-al [10] developed analytical model serving for investigating the three-roll bending forming process including spring-back effects of WELDOX900 material and developed an analytical and FEA models well agreed with the experiments. They developed created 3-D FEA models to bend a plate into a semi-circular workpiece. They also presented another mathematical formula for the vertical displacement of the inner roller with unloaded radius after spring-back [17]. The spring-back radius and angle were also calculated in that study. They studied different three–roll bending machine models that had rollers with different sizes in ABAQUS software which was confirmed to be an optimum tool by experiments.

Feng & Champliaud [4] created both analytical and dynamic numerical models of an asymmetric three-roll bending process by using ANSYS/LS-DYNA [18], which is a commercial finite element analysis (FEA) software, and they analyzed the explicit FEA results by comparing them with experimental results.

Taking the heat into account, Quan et al. [16,19] conducted a set of thermo-mechanical FEA analyses through 3D explicit dynamic models by using ANSYS/ Ls-Dyna. They first discussed an analytical model developed by Salem [3,20] previously by including elastic deformation, elastic-perfectly plastic and elastoplastic deformation zones [16].

In the literature, the research studies related to ED-FEA models have mostly considered cylindrical rollers and flat plates to study the roller bending process [21,22]. Even though different roller geometries such as concave and convex shapes are commonly applied at a certain level in bending machine designs to compensate the cylinders' deflections that affect the final curvature of a plate being bent, there is still a lack of investigation in terms of the effect of the convex geometric design of the rollers and a bending plate with special geometry. Any ED-FEA study including discussions related to the rolling speed and the mass scaling factor and conducted to investigate the effect of time step size has not been encountered in the literature even though such studies are as significant as a convergence study widely conducted while investigating the effects of the element sizes on the results.

In the ED-FEA models to simulate the rolling process, the rollers are always defined with SHELL elements and a rigid material whereas the plate is defined with SHELL elements and number of integration points through the thickness of the plate. The material of the sheet is defined as a non-linear material with an elasto-plastic behavior with isotropic hardening [14].

2. Roll Bending Process

As can be seen in Figure 1 and Figure 2, operation principles of three-roller and four-roller bending machines have essential differences. As schematically shown in Figure 1, the inner roller only moves up and down and it is idle (that is, it is not driven by a motor), while the outer rollers are driven to rotate but they are stagnant (that is, they do not move upward or downward). By displacement of the inner roller toward the plate, it moves down to the point where the pinch pressure applied to the bending plate was set at a certain pressure [5]. As graphically shown in Figure 2, the difference in four-roller bending machines is not only the number of rollers but also the motion of the outer (side) rollers. Initially, the side rollers are located as symmetric in the design even though they can pivot by swing independent from each other by means of a part called wing. Hence, the side rollers can apply the required force and moments onto the plate [7,21].

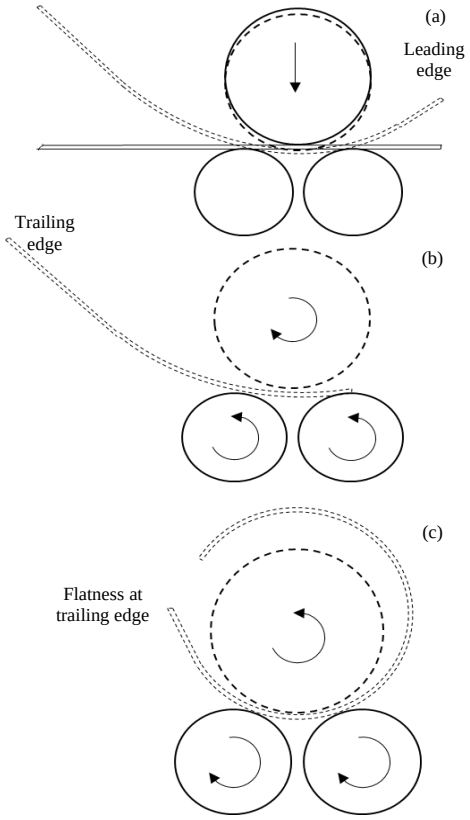

Figure 1. Schematic illustration of the steps of bending in a symmetric three roll quick rolling machine: (a) static bending (b) reverse pre-bending (c) forward bending

Four roll plate bending machines (Figure 3) that have higher efficiency compared to three roller machines are more commonly chosen by metal pipe manufacturers since they can have different operation modes to be able to carry out versatile functions. In another word, a four roll plate bending machine has two independent side rolls that can be moved upward and downward to be located for pre-bending and continuous bending processes in one pass from right to left or vice-versus. Thus, a fully circular geometry can be eventually obtained in different curvature sizes as desired (sequences 2 and 4 in Figure 2).

Hua et al [23–25]. conducted an elaborate study by developing a theoretical definition of the four-roll bending process comprehending the complete bending mechanism. Lin & Hua defined the sequences of bending as shown in Figure 2. The steady continuous roll-bending mode (sequences 4-6, Figure 2) is implemented to accomplish fully circular curvature in a certain diameter for the major portion of the part. The edge bending mode consisting of two sub-modes, edge pre-bending mode (sequence 2, Figure 2) and edge continuous roll-bending mode (sequence 3, Figure 2), has the function used to reduce the length of flat leading and trailing edges.

Springback concept and its analytical estimation in a metal forming [26] for its compensation in practice in die industry is of paramount importance in general as well as in the metal plate bending through both three-roller and four roller bending machines in particular. Springback can be defined as the elastically driven change of shape that occurs after deforming a plate at loading stage and then the plate tends to return to its original shape at unloading stage [21] and it partially returns due to the elasto-plastic deformation [5].

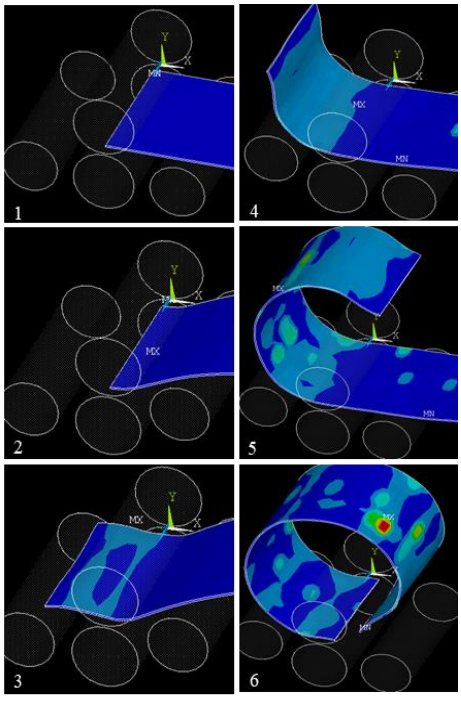

Figure 2. Sequence of four roll plate bending

3. Material and Methods

This study aims at developing a 3-D theoretical model using a non-linear explicit dynamics finite element model for a bending procedure of a metal plate with special geometry in a four roll bending machine (Figure 3). The FEA model is defined in detail so that it can be used for more generic cases of the continuous metal plate bending process. LS-DYNA solver in ANSYS Mechanical APDL (ANSYS Parametric Design Language) was employed as an explicit dynamic preprocessor for the generation of the two models including cylindrical as well as convex rollers. They were processed by Ls-Dyna solver engine and post-processor for analyses of the simulation results. In addition, since the discussion of the mass scaling factor, which significantly effects results as well as the computation cost, seems necessary and it should be included in any explicit dynamics model, this study takes into account the discussion of the peripheral velocity and mass scaling effects.

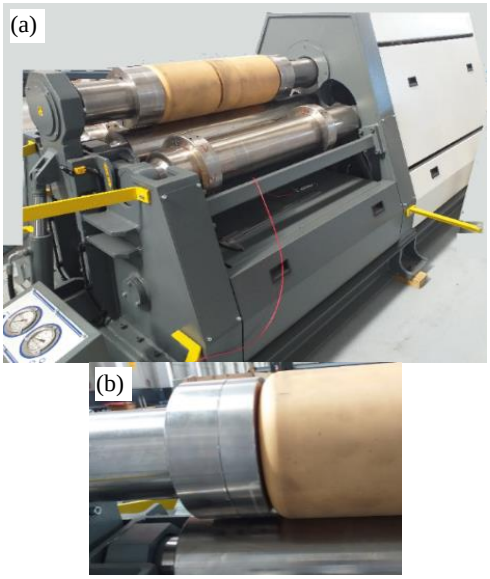

Figure 3. a) Four roll bending machine and b) the specific geometry of the top roller with channels

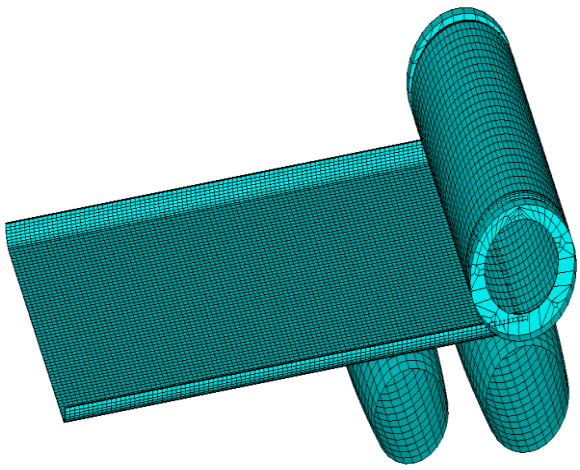

Figure 4. 3D meshed FEA model of asymmetric three roll bender for continuous bending of a plate

In the explicit non-linear dynamics FEA model, two different models were first generated in a commercial 3-D solid modeling software and then they were respectively imported into the ANSYS Mechanical APDL environment as step files in order to further generate the finite element models by defining; element types, mesh sizes, materials, contacts between the parts and motions with constraints.

Element types were defined as SOLID 164 for the Aluminum plate and SHELL 163 for the rollers' outer surfaces as listed in Table 1. After the solid model is imported into ANSYS, the model consists of areas and does not have volume. Before setting the SOLID 164 element type to the volumes and meshing them as illustrated in Figure 4, it is needed to convert areas that compose the plate into volumes and combine the generated volumes through the VGLUE command. Since shell element can be appointed to the areas, no conversion of the areas of the rollers is required to set the SHELL 163 to the certain roller areas.

Plate material is modeled by elasto-plastic Bilinear Kinematic Hardening model (Figure 5) through using the mechanical properties given in Table 2. To include the Bauschinger effect, it is assumed by the plasticity material model that the total stress range is equal to twice the yield stress. This model was chosen for the aluminum material since it met Von Mises yield criteria including the most metals. The tangent modulus is not able to take a value less than zero or its value cannot be greater than the value of elastic modulus [18]. The material properties were obtained from the tensile test data of the Al-552-H32 isotropic material depicted as the stress-strain graphic in Figure 5.

The three-roller materials were modeled as rigid steel materials as shown in Table 1, and their mechanical properties, as well as the transitional and rotational constraints, are presented in Table 2.

Contacts between each roller and the plate are defined as the general surface to surface contact with 0.3 static and dynamic friction coefficients. The real constant values for the shear factor and the number of integration points through the thickness of shell element of 1 mm are assumed to be 0.83 (5/6) and 5 respectively.

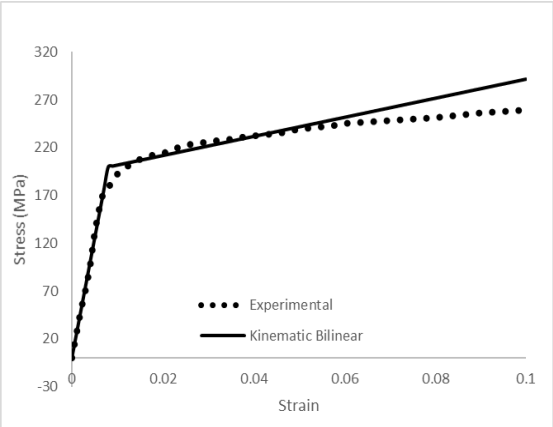

Figure 5. Kinematic Bilinear model and experimental Stress strain relation of Al-552-H32 material of the plate

Table 1 Material and element information for the parts of the model

Part	Mater.	Elem. type	Model 1: Elem. #	Model 2: Elem. #
1	Al	SOLID 164	15200	11400
2	Steel	SHELL 163	624	676
3	Steel	SHELL 163	728	780
4	Steel	SHELL 163	3193	3825

To bend the plate at desired diameter, the side roller is required to move upward at a certain distance and a certain speed. For this study, the coordinate of its final stop is (60.8; 15.49) in mm along y and z directions. The velocity of the side roller is supposed to be 10 mm/s. The duration of the transitional motion of the side roll from its velocity is defined as follows:

$$v_{SRoll} = 10 \text{ mm/s} \tag{1}$$

$$\tan\alpha = \frac{60.8}{15.49} \tag{2}$$

$$\alpha = 75.7^{\circ} \tag{3}$$

$$v_z = -10\,\text{Cos}\,\alpha = -2.4699 \text{ m/s} \tag{4}$$

$$v_y = -10\,\text{Sin}\,\alpha = 9.69 \text{ m/s} \tag{5}$$

$$t = \frac{y}{|v_y|} = \frac{60.8}{9.69} = 6.27 \text{ s} \tag{6}$$

or

$$t = \frac{z}{|v_z|} = \frac{15.49}{2.4699} = 6.27 \text{ s} \tag{7}$$

The angular velocity of the upper roll rotation ω_{TRoll} is determined as 0.72 rad/s (equals to 5000 mm/min of its peripheral velocity, v_{TRoll}) for the first set of the FEA simulations. The relation between the ω_{TRoll} and v_{TRoll} is as the following algebraic procedure;

$$v_{TRoll} = 5000 \text{ mm/min} \tag{8}$$

$$n = \frac{v_{TRoll}}{\pi D} = \frac{5000 \text{ mm/min}}{\pi.230 \text{ mm}} = 6.92 \text{ rpm} \tag{9}$$

$$\omega = \frac{2\pi n}{60} = 0.72 \text{ rad/s} \tag{10}$$

3.1 FEA Model with Cylindrical Rollers

In the first model, as shown in Figure 6, the bottom roller and the side roller are defined as cylinders with diameters of Ø210 mm and Ø190 mm, respectively. The top roller is Ø230 mm cylinder and has channels with a certain depth on its two ends for insertion of the side walls of the aluminum plate as depicted in Figure 6. The thickness of the aluminum plate was chosen as 3.175 mm, the width from outer surface of the side wall to that of the other side wall as 635 mm, and the length as 1000 mm. In this research, we aim at finding out a suitable design for the four roll bending machine and set a proper rotation velocity of the upper roll to achieve bending without any failure. It is a challenging task to accomplish the

bendability with a neat final circular geometry due to the pre-bent side walls of the aluminum plate.

3.2 FEA Model with Convex Rollers

Although it was not possible to eliminate the material failure that occurred during the beginning of the bending process, to minimize it, the design of the bottom and the side rolls was changed to convex geometry as shown in Figure 7.

The diameters of the bottom pinch roll were defined as Ø180-Ø210 mm and that of the side roll as Ø160-Ø190 mm. The top roll design remained the same.

The computation time and accuracy of the results should be optimized by conducting a convergence study. Conducting explicit dynamic analyses is costly in terms of computation time in order to obtain accurate results.

Ls-Dyna solver is the best-fit and the most convenient software for such analyses. For a low-velocity metal forming process done through ED-FEA, the computation time and the results are affected by the time step size. To be able to minimize the computation cost, the element size can be set by the Mesh Tool assigning to a specific size for critical edges or zones usually relatively smaller in comparison to non-critical ones. Another effective method is mass scaling. The use of mass scaling, as explained in detail in the Appendix section, can be very helpful, especially in the low-velocity simulations such as that of roll-bending of a plate. It is useful in situations in which more intensively meshing of an area of interest is needed.

First, a 3-D FEA model including cylindrical rollers was created and a pre-bending simulation with top roller not being rotated was conducted only to validate the model by comparing it with the experimental results. In the FEA model, the mass scaling was assigned as $4x10^{-6}$. The element sizes along the width and the length of the plate were chosen to be 25mm; however, the element size along the thickness – that is critical to simulate the bending phenomenon – was chosen to be much smaller (5 elements along the thickness of 3.175 mm) in comparison to other dimensions of the plate.

4. Result and Discussion

4.1 Influence of Side Walls of the Plate

As seen in Figure 9(a), the aluminum plate experiences various deformation forms at different time spots as the plate is being bent. The nodal deformation list in Y direction along the rear edge of the plate was extracted as *csv* data file and plotted in Excel. The results are also illustrated in 2-D graphics in terms of the nodal deformation of the rear edge of the plate in mm as shown in Figure 9 (b). The deformation of the plate becomes concave and then takes a convex form similar to the experimental result as shown in Figure 10. The distortion has occurred only on one side wall in both FEA (Figure 11) and experimental results (Figure 10). These conclude that the FEA model very closely predicts the reality of the bending phenomena of an aluminum fender by a four-roll bending machine. Therefore, the low-velocity non-linear explicit FEA model could be considered for different parameters in a future parametric study.

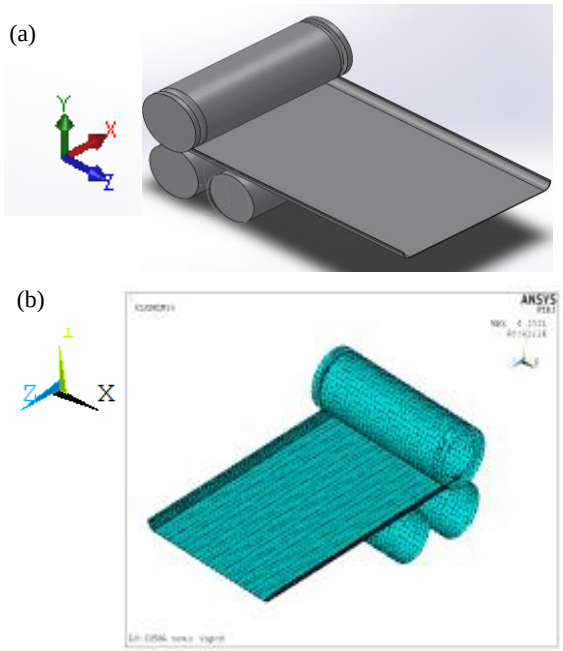

Figure 6. Three-dimensional a) solid model and b) meshed model of asymmetric three roll bending

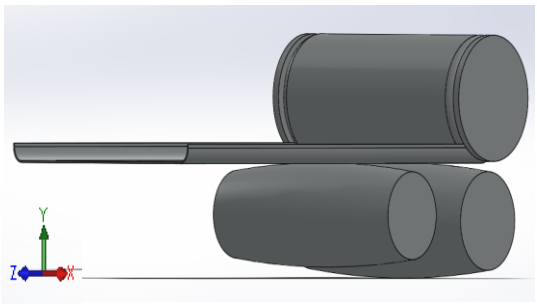

Figure 7. Three-dimensional solid model of asymmetric three roll bender with convex side and bottom roller

Table 2. Material models of the aluminum plate and the rollers

Material	Model	Density (kg/mm^3)	Young's Modulus (MPa)	Poisson Ratio	Yield Stress (MPa)	Tangent Modulus (MPa)	Translational Constraint	Rotational Constraint
Alum. Plate	Bilinear Kinem.	2.68×10^{-6}	70300	0.33	193	750		
Side roll	Rigid	7.8×10^{-6}	210000	0.3			X Disp.	All Rot.
Bottom roll	Rigid	7.8×10^{-6}	210000	0.3			All Disp.	All Rot.
Top roll	Rigid	7.8×10^{-6}	210000	0.3			All Disp.	All Rot.

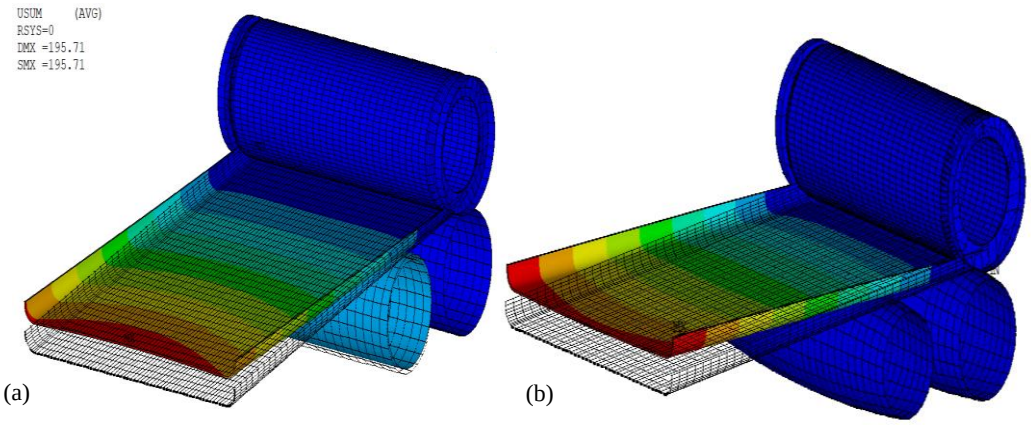

Figure 8. Demonstration of two models with a) cylindrical rollers and b) convex side and bottom rollers

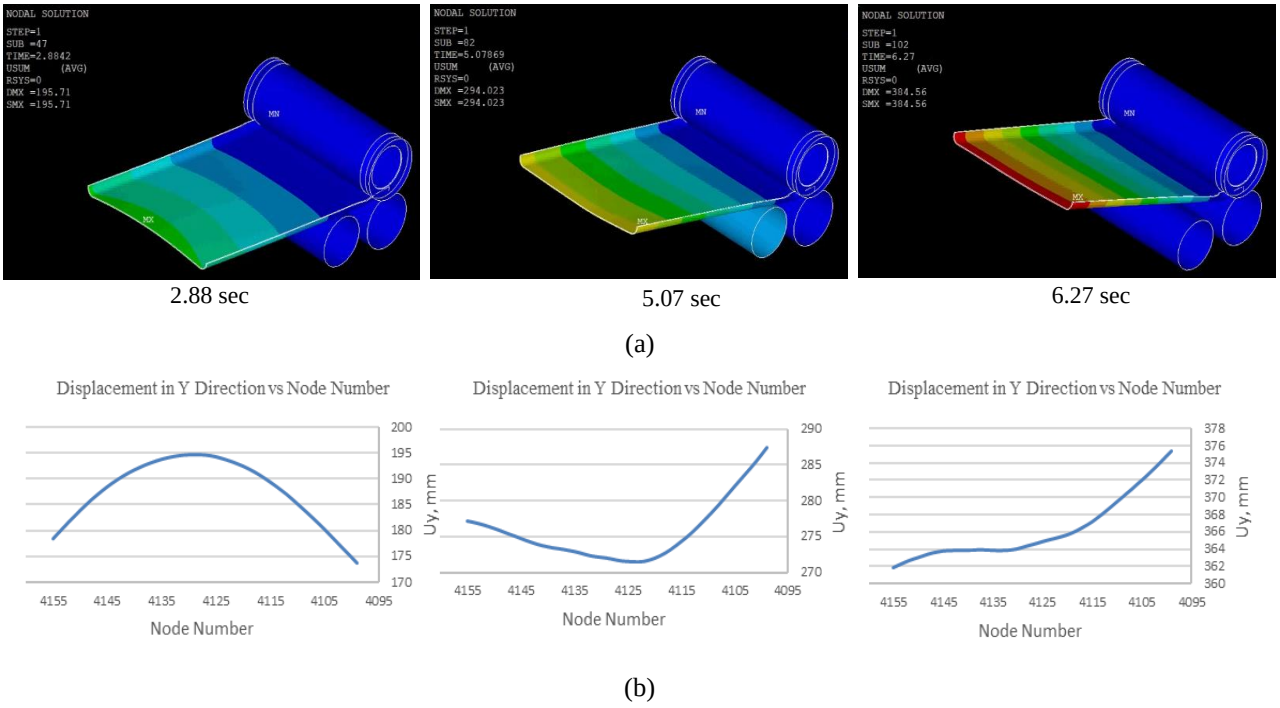

Figure 9. Demonstration of the deformation results from the cylindrical roller model in a) contour plots and b) 2-D plots of the displacements along the nodes of the rear edge of the aluminum plate at different time spot

4.2 Influence of Top Roller Rotation Speed During Bending

The design of the bottom and side roller geometries was changed to convex. The new design was tried in another FEA simulation to avoid the experimental cost with regards to a lot of scraps. Because the previous FEA model in Ls-Dyna accomplished to predict the experimental results obtained from the cylindrical rollers, another FEA simulation was conducted with the 3D model involving convex rollers. In this simulation, the top roller was rotated with the peripheral velocity of 5000 mm/min (angular velocity of 0.72 rad/s) and the mass scaling factor was doubled in a way to be 8x10-6 for the sake of reducing the computational cost in half. Although the bottom and side roller geometry were changed to convex with the sizes given in the previous section, the top roller design was not changed.

4.3 Influence of convex rollers during pre-bending

Since the distortion still seemed too much, the rotation speed was presumed as the reason and the rotational speed of the top roller was reduced to 0.18 rad/s, the element size along the length and the width of the plate was reduced to 10 mm, and the rest of the model remained the same. The design change of the bottom and side rollers and the reduction of the top roller speed did not work out as expected. The distortion could be neither avoided nor reduced as the plate being bent by a four roller plate bending machine as can be seen in Figure 12. Therefore, a completely different methodology could be studied in the future to accomplish the bending of a fender with two side walls.

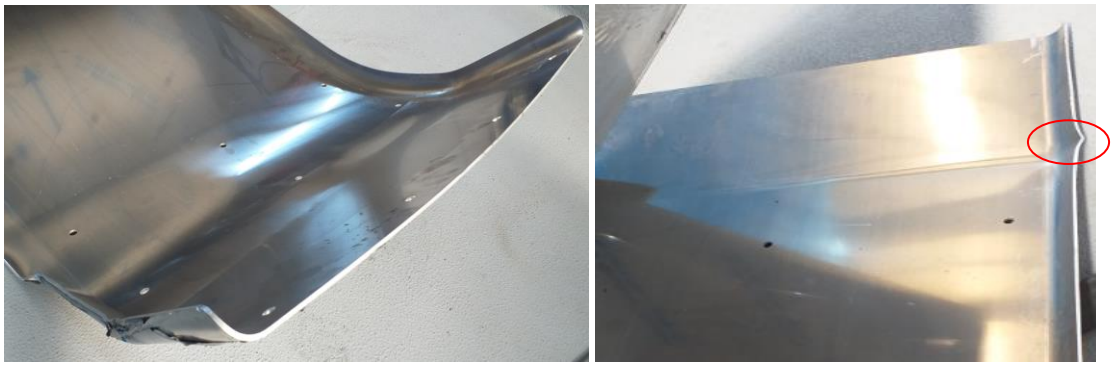

Figure 10. Demonstration of the experimental deformation results

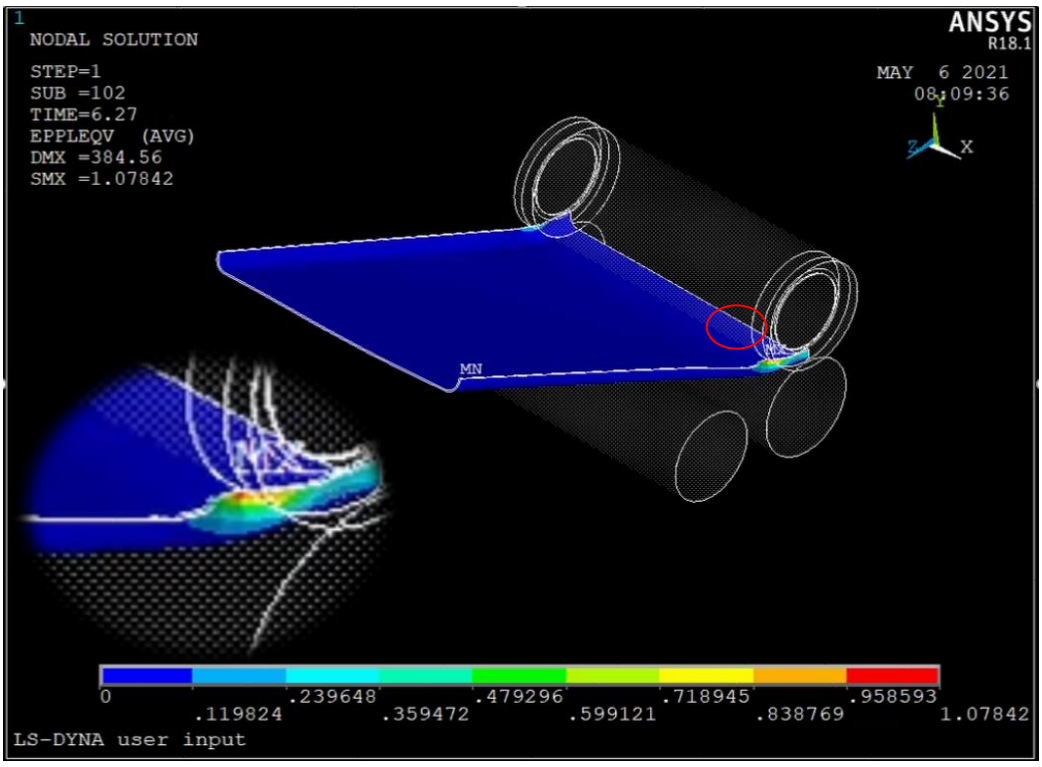

Figure 11. Demonstration of the Von-Mises Equivalent stress results from the cylindrical roller model in contour graphs

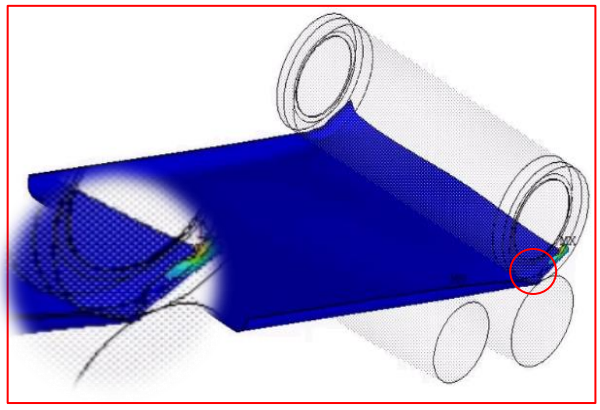

Figure 12. FEA results in terms of distortion of the side wall of the plate during bending

5. Conclusions

In this study, the explicit dynamics FEA model was created with two different 3-D models including cylindrical and convex geometries of bottom and side rollers. The FEA model was first validated with the experimental results. Since resembling deformation results was obtained, the FEA model with different parameters such as geometry, element size, mass scaling factor, and rotational speed was created in Ls-Dyna and simulated for different cases to avoid experimental trial and error costs such as scraps, labor, and time. In this study, the importance of the mass scaling factor to minimize computational cost was also discussed. It is used to increase the time step of the explicit dynamics simulation; however, one needs to pay attention that too much reduction of the simulation time results in unphysical consequences.

Unfortunately, the design change and speed reduction did not work out as not to avoid the distortion. Nevertheless, the results obtained in this study may shed light on a possible future study to be conducted on bending an aluminum fender with sidewalls such as two-step

forming process involving roll bending and then roll forming or vice-versus.

For the researchers in the metal-forming field, this study also aimed to present a comprehensive explanation for an explicit dynamics FEA simulation of roll-bending of a plate and creation of a 3-D model with the significant parameters such as mass scaling and element size used to control for optimization between the prediction accuracy and the computational cost. In a simple static structural analysis, a convergence analysis with regards to the element size might be sufficient to optimize an FEA model, however, once a highly costly non-linear dynamic analysis is considered, the time step must be also taken into account more carefully to attain physical and accurate results

Declaration

The author(s) declared no potential conflicts of interest with respect to the research, authorship, and/or publication of this article. The author(s) also declared that this article is original, was prepared in accordance with international publication and research ethics, and ethical committee permission or any special permission is not required.

Author Contributions

F. Author performed the analysis and developed the methodology. S. Author supervised and improved the 3-D model.

Nomenclature

α : The angle of transitional motion of the side roller

c : The sonic velocity

E : Young's (Elasticity) Modulus

ρ : The material density

n : The rotation count per minute

υ : Poisson's ratio

Δt : The time step size

t : The time

v_{SRoll} : The transitional velocity of the side roller

v_{TRoll} : The peripheral velocity of the top roller

ω : The angular velocity

References

1. Zeng, J., Z. Liu, and H. Champliaud, *FEM dynamic simulation and analysis of the roll-bending process for forming a conical tube*, Journal of Materials Processing Technology, 2008. **198:** p. 330–343.
2. Gandhi, A.H. and H.K. Raval, *Analytical and empirical modeling of top roller position for three-roller cylindrical bending of plates and its experimental verification*, Journal of Materials Processing Technology, 2008. **197:** p. 268–278.
3. Salem, J., H. Champliaud, Z. Feng, and T.M. Dao, *Experimental analysis of an asymmetrical three-roll bending process*, International Journal of Advanced Manufacturing Technology, 2016. **83:** p. 1823–1833.
4. Feng, Z. and H. Champliaud, *Modeling and simulation of asymmetrical three-roll bending process*, Simulation Modelling Practice and Theory, 2011. **19:** p. 1913–1917.
5. Shinkin, V.N., *Asymmetric three-roller sheet-bending systems in steel-pipe production*, Steel in Translation, 2017. **47:** p. 235–240.
6. Wang, Y., X. Zhu, Q. Wang, and X. Cui, *Research on multi-roll roll forming process of thick plate*, International Journal of Advanced Manufacturing Technology, 2019. **102:** p. 17–26.
7. Wu, K., Y. Sun, C. Cao, C. Zhou, Q. Liu, and X. Chang, *On Simulation Analysis of Plate Forming and Deformation Compensation Technology of the side roll for Four-roll Plate Bending Machine*, Procedia Engineering, 2017. **207:** p. 1617–1622.
8. Hua, M., K. Baines, and D.H. Sansome, *Design and Performance Considerations of the Continuos Four-roll Bender: A Precision Machine for the Roller Bending of Plates*, Progress in Precision Engineering, 1991. p. 277–289.
9. Chudasama, M.K. and H.K. Raval, *Bending force prediction for dynamic roll-bending during 3-roller conical bending process*, Journal of Manufacturing Processes, 2014. **16:** p. 284–295.
10. Fu, Z., X. Tian, W. Chen and B. Hu, *Analytical modeling and numerical simulation for three-roll bending forming of sheet metal*, Int J Adv Manuf Technol, 2013. p. 1639–1647.
11. Tailor, V.K., A.H. Gandhi, R.D. Moliya and H.K. Raval, *Finite Element Analysis of Deformed Geometry in Three Roller Plate Bending Process*, in: International Manufacturing Science and Engineering Conference MSEC2008, Evanston, IL,USA, 2018. p. 1–8.
12. Zhigulev, G.P., M.N. Skripalenk, V.A. Fadeev, and M.M. Skripalenko, *Modeling of Deformation Zone during Plate Stock Molding in Three-Roll Plate Bending* Machine, Metallurgist, 2020. **64:** p. 348–355.
13. Amiolemhen, P.E. and J.K. Abiegbe, *Design and Fabrication of a Three - Rolls Plate Bending Machine*, Innovative Systems Design and Engineering, 2019. **10:** p. 31–41.
14. Boazu, I., D. and F. Stan, *Estimating of bending force and curvature of the bending plate in a three-roller bending system using finite element simulation and analytical modeling*, Materials, 2021. **14:** p 1–16.
15. Gavrilescu, I. and D. Boazu, *Simulation of Roll Bending with Three Rollers Pyramid System Using FEM*, 2017. p. 21–28.
16. Tran, Q.H., H. Champliaud, Z. Feng, and T.M. Dao, *Analysis of the asymmetrical roll bending process through dynamic FE simulations and experimental study*, International Journal of Advanced Manufacturing Technolog, 2014. **75:** p. 1233–1244.
17. Burchitz, I., *Springback: improvement of its predictability: Literature study report*, 2005. p. 49–62.
18. ANSYS/LS-DYNA Help, (2018).
19. Quan, T.H., H. Champliaud, Z. Feng, J. Salem, D.T. My, *Heat-assisted roll-bending process dynamic simulation*, International Journal of Modelling and Simulation, 2013. **33:** p. 54–62.
20. Salem, J., ©Tous droits réservés, Jamel Salem, 2012.
21. G. Yu, J. Zhao, C. Xu, *Development of a symmetrical four-roller bending process*, International Journal of Advanced Manufacturing Technology, 2019. **104:** p. 4049–4061.
22. Quan, T.H., H. Champliaud, Z. Feng, and D. Thien-My,

Dynamic analysis of a workpiece deformation in the roll bending process by FEM simulation, 24th European Modeling and Simulation Symposium, EMSS 2012. p. 477–482.

23. Lin, Y.H. and M. Hua, *Influence of strain hardening on continuous plate roll-bending process,* International Journal of Non-Linear Mechanics, 2000. **35:** p. 883–896.
24. Hua, M., I.M. Cole, K. Baines, and K.P. Rao, *A formulation for determining the single-pass mechanics of the continuous four-roll thin plate bending process,* Journal of Materials Processing Technology, 1997. **67:** p. 189–194.
25. Hua, M., K. Baines, and I.M. Cole, *Continuous four-roll plate bending: A production process for the manufacture of single seamed tubes of large and medium diameters,* International Journal of Machine Tools and Manufacture. 1999. **39:** p. 905–935.
26. Wagoner, R.H., J.F. Wang, M. Li, and T. Ohio, *Springback,* 2006. p. 1–23.

Appendix

The Mass Scaling increases the required time step by increasing the mass of the minimum sized elements. In conditions where the low velocity analysis type is conducted, the mass scaling is better to be switched on, and in the Hourglass effect, the type 6 can be chosen for the low-velocity analyses. For explicit time integration, the minimum time step-size depends on the minimum element length ($l_{\min}$) and the sonic speed (c). Note that, in the model, the smallest element size controls the minimum time step size ($\Delta t_{\min}$) for a given set of material properties. In addition, for a certain mesh, the minimum time step size varies based on the sonic speed that is a function of material properties:

$$\Delta t_{\min} = \frac{l_{\min}}{c} \tag{A1}$$

$$c = \sqrt{\frac{E}{\left(1-\upsilon^2\right)\rho}} \tag{A2}$$

where υ is the Poisson's ratio, E is the Young's modulus, and ρ is the density.

In the ANSYS LS-DYNA software, the minimum time step size can be controlled through including mass scaling into the analysis process. To be able to reduce the temporal cost, the mass scaling criterion must be used when the time-step calculated by the software is too minimal. In conditions where the mass scaling is specified, element density is set to reach a pre-defined time step size Δt_{sp} with the following equation:

$$\rho_i = \frac{{\Delta t_{sp}}^2 E}{l_i^2\left(1-\upsilon^2\right)} \tag{A3}$$